

Forward-backward asymmetries in $\Lambda_b \rightarrow \Lambda l^+ l^-$ in the Bethe-Salpeter equation approach*

Liang-Liang Liu(刘亮亮)^{1†} Su-Jun Cui(崔苏君)¹ Jing Xu(徐晶)² Xin-Heng Guo(郭新恒)^{3‡}

¹College of Physics and information engineering, Shanxi Normal University, Taiyuan 030031, China

²Department of Physics, Yan-Tai University, Yantai 264005, China

³College of Nuclear Science and Technology, Beijing Normal University, Beijing 100875, China

Abstract: Using the Bethe-Salpeter equation (BSE), we investigate the forward-backward asymmetries (A_{FB}) in $\Lambda_b \rightarrow \Lambda l^+ l^- (l = e, \mu, \tau)$ in the quark-diquark model. This approach provides precise form factors that are different from those of quantum chromodynamics (QCD) sum rules. We calculate the rare decay form factors for $\Lambda_b \rightarrow \Lambda l^+ l^-$ and investigate the (integrated) forward-backward asymmetries in these decay channels. We observe the integrated A_{FB}^l , $\bar{A}_{FB}^l(\Lambda_b \rightarrow \Lambda e^+ e^-) \approx -0.1371$, $\bar{A}_{FB}^l(\Lambda_b \rightarrow \Lambda \mu^+ \mu^-) \approx -0.1376$, and $\bar{A}_{FB}^l(\Lambda_b \rightarrow \Lambda \tau^+ \tau^-) \approx -0.1053$; the hadron side asymmetries $\bar{A}_{FB}^h(\Lambda_b \rightarrow \Lambda \mu^+ \mu^-) \approx -0.2315$; the lepton-hadron side asymmetries $\bar{A}_{FB}^{lh}(\Lambda_b \rightarrow \Lambda \mu^+ \mu^-) \approx 0.0827$; and the longitudinal polarization fractions $F_L(\Lambda_b \rightarrow \Lambda \mu^+ \mu^-) \approx 0.5681$.

Keywords: rare decay, Bethe-Salpeter equation, heavy flavor physics

DOI: 10.1088/1674-1137/ac7041

I. INTRODUCTION

The decays of hadrons involving the flavor changing neutral current (FCNC) transition such as $\Lambda_b \rightarrow \Lambda l^+ l^-$ can provide essential information about the inner structure of hadrons, reveal the nature of the electroweak interaction, and provide model-independent information about physical quantities such as Cabibbo-Kobayashi-Maskawa (CKM) matrix elements. The rare decay $\Lambda_b \rightarrow \Lambda \mu^+ \mu^-$ was first observed by the CDF collaboration in 2011 [1]. Some experimental progress on $\Lambda_b \rightarrow \Lambda l^+ l^-$ was also achieved [2–5], and the radiative decay $\Lambda_b \rightarrow \Lambda \gamma$ was observed in 2019 [3] by the LHCb collaboration. The LHCb collaboration determined the forward-backward asymmetries (A_{FB}^l) of the decay $\Lambda_b \rightarrow \Lambda \mu^+ \mu^-$ to be $A_{FB}^l(\Lambda_b \rightarrow \Lambda \mu^+ \mu^-) = -0.05 \pm 0.09$ (stat) ± 0.03 (syst), $A_{FB}^h(\Lambda_b \rightarrow \Lambda \mu^+ \mu^-) = -0.29 \pm 0.09$ (stat) ± 0.03 (syst), and $F_L(\Lambda_b \rightarrow \Lambda \mu^+ \mu^-) = 0.61^{+0.11}_{-0.14} \pm 0.03$ (syst) at the low dimuon invariant mass squared range $15 < q^2 < 20$ GeV 2 in 2015 [4]. However, these numbers were updated in 2018 to $\bar{A}_{FB}^l(\Lambda_b \rightarrow \Lambda \mu^+ \mu^-) = -0.39 \pm 0.04$ (stat) ± 0.01 (syst), $A_{FB}^h(\Lambda_b \rightarrow \Lambda \mu^+ \mu^-) = -0.3 \pm 0.05$ (stat) ± 0.02 (syst), and $\bar{A}_{FB}^{lh}(\Lambda_b \rightarrow \Lambda \mu^+ \mu^-) = 0.25 \pm 0.04$ (stat) ± 0.01 (syst) in

the same invariant mass squared region [5]. Note that A_{FB}^l is significantly larger than the previous one. In this study, we investigate the A_{FB} of $\Lambda_b \rightarrow \Lambda l^+ l^-$ in the Bethe-Salpeter equation (BSE) approach. Theoretically, only a few studies have been conducted on $A_{FB}(\Lambda_b \rightarrow \Lambda l^+ l^-)$ [6–17]. References [6] ([7]) provided the integrated forward-backward asymmetries $\bar{A}_{FB}^l(\Lambda_b \rightarrow \Lambda \mu^+ \mu^-) = -0.13$ (-0.12) and $\bar{A}_{FB}^l(\Lambda_b \rightarrow \Lambda \tau^+ \tau^-) = -0.04$ (-0.03), whereas the results of Ref. [8] were $\bar{A}_{FB}^l(\Lambda_b \rightarrow \Lambda e^+ e^-) = 1.2 \times 10^{-8}$, $\bar{A}_{FB}^l(\Lambda_b \rightarrow \Lambda \mu^+ \mu^-) = 8 \times 10^{-4}$, and $\bar{A}_{FB}^l(\Lambda_b \rightarrow \Lambda \tau^+ \tau^-) = 9.6 \times 10^{-4}$. Ref. [10] analyzed the differential $\bar{A}_{FB}(\Lambda_b \rightarrow \Lambda l^+ l^-)$ in the heavy quark limit. Using the non-relativistic quark model, Ref. [11] investigated the lepton-side forward-backward asymmetries $\bar{A}_{FB}^l(\Lambda_b \rightarrow \Lambda l^+ l^-)$. In the quark-diquark model, Ref. [12] investigated the lepton-side forward-backward asymmetries A_{FB} , the hadron-side forward-backward asymmetries A_{FB}^h , and the hadron-lepton forward-backward asymmetries A_{FB}^{hl} . In an approach of the light-cone sum rules, Refs. [13, 14] investigated the rare decays of $\Lambda_b \rightarrow \Lambda \gamma$ and $\Lambda_b \rightarrow \Lambda l^+ l^-$. Ref. [15] investigated the phenomenological potential of the rare decay $\Lambda_b \rightarrow \Lambda l^+ l^-$ with a subsequent, self-analyzing $\Lambda_b \rightarrow N\pi$ transition. With the form factors (FFs) ex-

Received 8 March 2022; Accepted 17 May 2022; Published online 26 July 2022

* Supported by National Natural Science Foundation of China (11905117, 11775024)

† E-mail: liu06_04@sxnu.edu.cn

‡ E-mail: xhguo@bnu.edu.cn



Content from this work may be used under the terms of the Creative Commons Attribution 3.0 licence. Any further distribution of this work must maintain attribution to the author(s) and the title of the work, journal citation and DOI. Article funded by SCOAP³ and published under licence by Chinese Physical Society and the Institute of High Energy Physics of the Chinese Academy of Sciences and the Institute of Modern Physics of the Chinese Academy of Sciences and IOP Publishing Ltd

tracted from a constituent quark model, Ref. [16] investigated the rare weak dileptonic decays of the Λ_b baryon. Ref. [17] studied $\mathcal{B}_1 \rightarrow \mathcal{B}_2 l^+ l^-$ ($\mathcal{B}_{1,2}$ are spin 1/2 baryons) with the $SU(3)$ flavor symmetry. The FFs of $\Lambda_b \rightarrow \Lambda$ differ in different models. Generally, the number of independent FFs of $\Lambda_b \rightarrow \Lambda$ can be reduced to 2 when working in the heavy quark limit [18],

$$\langle \Lambda(p) | \bar{s} \Gamma b | \Lambda_b(v) \rangle = \bar{u}_\Lambda(F_1(q^2) + F_2(q^2) \not{v}) \Gamma u_{\Lambda_b}(v), \quad (1)$$

where $\Gamma = \gamma_\mu, \gamma_\mu \gamma_5, q^\nu \sigma_{\nu\mu},$ and $q^\nu \sigma_{\nu\mu} \gamma_5$, q^2 is the square of the transformed momentum. The FF ratio $R(q^2) = F_2(q^2)/F_1(q^2)$ was considered a constant in many studies assuming the same shape for F_1 and F_2 , and it was derived from quantum chromodynamics (QCD) sum rules in the framework of the heavy quark effective theory [6]. For example, in Refs. [6, 7] the q^2 dependence of FF F_i ($i = 1, 2$) were given as follows:

$$F_i(q^2) = \frac{F_i(0)}{1 - aq^2 + bq^4}, \quad (2)$$

where a and b are constants. Using experimental data for the semileptonic decay $\Lambda_c \rightarrow \Lambda e^+ \nu_e$ ($m_\Lambda^2 \leq q^2 \leq m_{\Lambda_c}^2$), the CLEO collaboration provided the ratio $R = -0.35 \pm 0.04$ (stat) ± 0.04 (syst) [19]. In Ref. [20], the authors investigated $\Lambda_b \rightarrow \Lambda \gamma$ obtaining $R = -0.25 \pm 0.14 \pm 0.08$. In Refs. [6, 7, 21], the authors investigated the baryonic decay $\Lambda_b \rightarrow \Lambda l^+ l^-$ and obtained $R = -0.25$. In Ref. [22], the relation $F_2(q^2)/F_1(q^2) \approx F_2(0)/F_1(0)$ was given. However, according to the pQCD scaling law [23–25], the FFs should not have the same shape. Using Stech's approach, Ref. [26] obtained the FF ratio $R(q^2) \propto -1/q^2$. From the data in Ref. [27], we can estimate the value of R and observe that it changes from -0.83 to -0.32 , which is not a constant. In our previous studies [28, 29], we observed that the ratio R is not a constant in the Λ_b rare decay in a large momentum region in which we did not consider the long distance contributions because they have a small effect on the FFs of this decay [30, 31]. In these studies, Λ_b (Λ) was considered a bound state of two particles: a quark and a scalar diquark. This model has been used to study many heavy baryons [32]. Using the kernel of the

BSE, including scalar confinement and one-gluon-exchange terms and the covariant instantaneous approximation, we obtained the Bethe-Salpeter (BS) wave functions of Λ_b and Λ [28, 29]. In this study, we recalculate the FFs of $\Lambda_b \rightarrow \Lambda$ in this model.

The remainder of this paper is organized as follows. In Sec. II, we derive the general FFs and A_{FB} for $\Lambda_b \rightarrow \Lambda l^+ l^-$ in the BS equation approach. In Sec. III, the numerical results for A_{FB} and \bar{A}_{FB} of $\Lambda_b \rightarrow \Lambda l^+ l^-$ are provided. Finally, the summary and discussion are presented in Sec. V.

II. THEORETICAL FORMALISM

A. BSE for $\Lambda_b(\Lambda)$

As shown in Fig. 1, following our previous research, the BS amplitude of $\Lambda_b(\Lambda)$ in momentum space satisfies the integral equation [28, 29, 33–39]

$$\chi_P(p) = S_F(\lambda_1 P + p) \int \frac{d^4 q}{(2\pi)^4} K(P, p, q) \chi_P(q) S_D(\lambda_2 P - p), \quad (3)$$

where $K(P, p, q)$ is the kernel, which is defined as the sum of the two particles irreducible diagrams, S_F and S_D are the propagators of the quark and scalar diquark, respectively. $\lambda_{1(2)} = m_{q(D)}/(m_q + m_D)$, where $m_{q(D)}$ is the mass of the quark (diquark), and P is the momentum of the baryon.

We assume the kernel has the following form:

$$-iK(P, p, q) = I \otimes IV_1(p, q) + \gamma_\mu \otimes (p_2 + q_2)^\mu V_2(p, q), \quad (4)$$

where V_1 results from the scalar confinement, and V_2 is from the one-gluon-exchange diagram. According to the potential model, V_1 and V_2 have the following forms in the covariant instantaneous approximation ($p_l = q_l$) [28, 29, 37–39]:

$$\begin{aligned} \hat{V}_1(p_t - q_t) &= \frac{8\pi\kappa}{[(p_t - q_t)^2 + \mu^2]^2} - (2\pi)^2 \delta^3(p_t - q_t) \\ &\times \int \frac{d^3 k}{(2\pi)^3} \frac{8\pi\kappa}{(k^2 + \mu^2)^2}, \end{aligned} \quad (5)$$

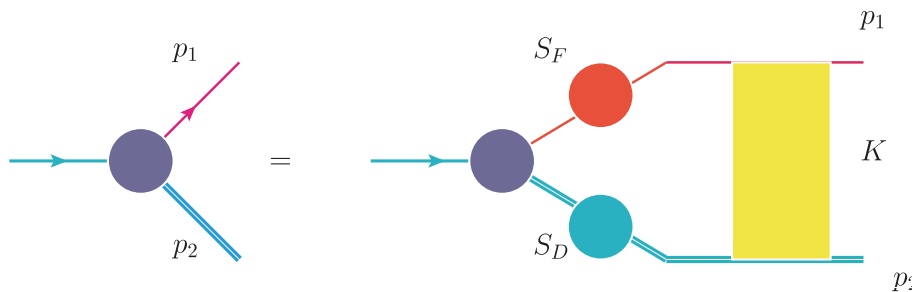


Fig. 1. (color online) BS equation for $\Lambda_b(\Lambda)$ in momentum space (K is the interaction kernel)

$$\tilde{V}_2(p_t - q_t) = -\frac{16\pi}{3} \frac{\alpha_{\text{eff}}^2 Q_0^2}{[(p_t - q_t)^2 + \mu^2][(p_t - q_t)^2 + Q_0^2]}, \quad (6)$$

where μ is a small parameter; to avoid the divergence in numerical calculation, this parameter is considered to be sufficiently small such that the results are not sensitive to it. The parameters κ and α_{eff} are related to scalar confinement and the one-gluon-exchange diagram, respectively. q_t is the transverse projection of the relative momentum along the momentum P , which is defined as $p_l = \lambda_1 P - v \cdot p$, $p_t^\mu = p^\mu - (v \cdot p)p^\mu$ ($v^\mu = P^\mu/M$), $q_t^\mu = q^\mu - (v \cdot q)v^\mu$, and $q_l = \lambda_2 P - v \cdot q$. The second term of \tilde{V}_1 is introduced to avoid infrared divergence at the point $p_t = q_t$, and μ is a small parameter to avoid the divergence in numerical calculations. Analyzing the electromagnetic FFs of the proton, $Q_0^2 = 3.2 \text{ GeV}^2$ was observed to provide consistent results with the experimental data [40].

The propagators of the quark and diquark can be expressed as follows:

$$S_F(p_1) = i \not{p} \left[\frac{\Lambda_q^+}{M - p_l - \omega_q + i\epsilon} + \frac{\Lambda_q^-}{M - p_l + \omega_q - i\epsilon} \right], \quad (7)$$

$$S_D(p_2) = \frac{i}{2\omega_D} \left[\frac{1}{p_l - \omega_D + i\epsilon} - \frac{1}{p_l + \omega_D - i\epsilon} \right], \quad (8)$$

where $\omega_q = \sqrt{m^2 - p_t^2}$ and $\omega_D = \sqrt{m_D^2 - p_t^2}$, M is the mass of the baryon, and Λ^\pm are the projection operators, which are defined as

$$2\omega_q \Lambda_q^\pm = \omega_q \pm \not{p} (p_l + m), \quad (9)$$

and satisfy the following relations:

$$\Lambda_q^\pm \Lambda_q^\pm = \Lambda_q^\pm, \quad \Lambda_q^\pm \Lambda_q^\mp = 0. \quad (10)$$

Generally, we require two scalar functions to describe the BS wave function of $\Lambda_b(\Lambda)$ [33–35],

$$\chi_P(p) = (f_1(p_t^2) + \not{p} f_2(p_t^2)) u(P), \quad (11)$$

where f_i ($i = 1, 2$) are the Lorentz-scalar functions of p_t^2 , and $u(P)$ is the spinor of a baryon.

Defining $\tilde{f}_{1(2)} = \int \frac{dp_l}{2\pi} f_{1(2)}$, and using the covariant instantaneous approximation, the scalar BS wave functions satisfy the following coupled integral equations:

$$\tilde{f}_1(p_t) = \int \frac{d^3 q_t}{(2\pi)^3} M_{11}(p_t, q_t) \tilde{f}_1(q_t) + M_{12}(p_t, q_t) \tilde{f}_2(q_t), \quad (12)$$

$$\tilde{f}_2(p_t) = \int \frac{d^3 q_t}{(2\pi)^3} M_{21}(p_t, q_t) \tilde{f}_1(q_t) + M_{22}(p_t, q_t) \tilde{f}_2(q_t), \quad (13)$$

where

$$\begin{aligned} M_{11}(p_t, q_t) = & \frac{(\omega_q + m)(\tilde{V}_1 + 2\omega_D \tilde{V}_2) - p_t \cdot (p_t + q_t) \tilde{V}_2}{4\omega_D \omega_q (-M + \omega_D + \omega_q)} \\ & - \frac{(\omega_q - m)(\tilde{V}_1 - 2\omega_D \tilde{V}_2) + p_t \cdot (p_t + q_t) \tilde{V}_2}{4\omega_D \omega_c (M + \omega_D + \omega_q)}, \end{aligned} \quad (14)$$

$$\begin{aligned} M_{12}(p_t, q_t) = & \frac{-(\omega_q + m)(q_t + p_t) \cdot q_t \tilde{V}_2 + p_t \cdot q_t (\tilde{V}_1 - 2\omega_D \tilde{V}_2)}{4\omega_D \omega_c (-M + \omega_D + \omega_c)} \\ & - \frac{(m - \omega_q)(q_t + p_t) \cdot q_t \tilde{V}_2 - p_t \cdot q_t (\tilde{V}_1 + 2\omega_D \tilde{V}_2)}{4\omega_D \omega_q (M + \omega_D + \omega_q)}, \end{aligned} \quad (15)$$

$$\begin{aligned} M_{21}(p_t, q_t) = & \frac{(\tilde{V}_1 + 2\omega_D \tilde{V}_2) - (-\omega_q + m) \left(1 + \frac{q_t \cdot p_t}{p_t^2} \right) \tilde{V}_2}{4\omega_D \omega_q (-M + \omega_D + \omega_q)} \\ & - \frac{-(\tilde{V}_1 - 2\omega_D \tilde{V}_2) + (\omega_q + m) \left(1 + \frac{q_t \cdot p_t}{p_t^2} \right) \tilde{V}_2}{4\omega_D \omega_q (M + \omega_D + \omega_q)}, \end{aligned} \quad (16)$$

$$\begin{aligned} M_{22}(p_t, q_t) = & \frac{(m - \omega_q)(\tilde{V}_1 + 2\omega_D \tilde{V}_2)) p_t \cdot q_t - p_t^2 (q_t^2 + p_t \cdot q_t) \tilde{V}_2}{4p_t^2 \omega_D \omega_q (-M + \omega_D + \omega_q)} \\ & - \frac{(m + \omega_q)(-\tilde{V}_1 - 2\omega_D \tilde{V}_2)) p_t \cdot q_t + p_t^2 (q_t^2 + p_t \cdot q_t) \tilde{V}_2}{4p_t^2 \omega_D \omega_q (M + \omega_D + \omega_q)}. \end{aligned} \quad (17)$$

When the mass of the b quark approaches infinity [32], the propagator of the b quark satisfies the relation $\not{p} S_F(p_1) = S_F(p_1)$ and can be reduced to

$$S_F(p_1) = i \frac{1 + \not{p}}{2(E_0 + m_D - p_l + i\epsilon)}, \quad (18)$$

where $E_0 = M - m - m_D$ is the binding energy. Thus, the BS wave function of Λ_b has the form $\chi_P(v) = \phi(p) u_{\Lambda_b}(v, s)$, where $\phi(p)$ is the scalar BS wave function [32], and the BS equation for Λ_b can be replaced by

$$\begin{aligned} \phi(p) = & - \frac{i}{(E_0 + m_D - p_l + i\epsilon)(p_l^2 - \omega_D^2)} \\ & \times \int \frac{d^4 q}{(2\pi)^4} (\tilde{V}_1 + 2p_l \tilde{V}_2) \phi(q). \end{aligned} \quad (19)$$

Generally, we can take E_0 to be about -0.14 GeV and κ to be about 0.05 GeV^3 [28, 29].

B. Asymmetries of $\Lambda_b \rightarrow \Lambda l^+ l^-$ decays

In the Standard Model, the $\Lambda_b \rightarrow \Lambda l^+ l^-$ ($l = e, \mu, \tau$) transitions are described by $b \rightarrow sl^+ l^-$ at the quark level. The Hamiltonian for the decay of $b \rightarrow sl^+ l^-$ is given by

$$\mathcal{H}(b \rightarrow sl^+ l^-) = \frac{G_F \alpha}{2\sqrt{2}\pi} V_{tb} V_{ts}^* \left[C_9^{\text{eff}} \bar{s} \gamma_\mu (1 - \gamma_5) b \bar{l} \gamma^\mu l \right. \\ \left. - i C_7^{\text{eff}} \bar{s} \frac{2m_b \sigma^{\mu\nu} q^\nu}{q^2} (1 + \gamma_5) b \bar{l} \gamma^\mu l \right]$$

$$+ C_{10} \bar{s} \gamma_\mu (1 - \gamma_5) b \bar{l} \gamma^\mu \gamma_5 l \Big], \quad (20)$$

where G_F is the Fermi coupling constant, α is the fine structure constant at the Z mass scale, V_{ts} and V_{tb} are the CKM matrix elements, q is the total momentum of the lepton pair, and C_i ($i = 7, 9, 10$) are the Wilson coefficients. $C_7^{\text{eff}} = -0.313$, $C_9^{\text{eff}} = 4.334$, $C_{10} = -4.669$ [41–43]. The relevant matrix elements can be parameterized in terms of the FFs as follows:

$$\langle \Lambda(P') | \bar{s} \gamma_\mu b | \Lambda_b(P) \rangle = \bar{u}_\Lambda(P') (g_1 \gamma^\mu + i g_2 \sigma^{\mu\nu} q_\nu + g_3 q^\mu) u_{\Lambda_b}(P), \\ \langle \Lambda(P') | \bar{s} \gamma_\mu \gamma_5 b | \Lambda_b(P) \rangle = \bar{u}_\Lambda(P') (t_1 \gamma^\mu + i t_2 \sigma^{\mu\nu} q_\nu + t_3 q^\mu) \gamma_5 u_{\Lambda_b}(P), \\ \langle \Lambda(P') | \bar{s} i \sigma^{\mu\nu} q^\nu b | \Lambda_b(P) \rangle = \bar{u}_\Lambda(P') (s_1 \gamma^\mu + i s_2 \sigma^{\mu\nu} q_\nu + s_3 q^\mu) u_{\Lambda_b}(P), \\ \langle \Lambda(P') | \bar{s} i \sigma^{\mu\nu} \gamma_5 q^\nu b | \Lambda_b(P) \rangle = \bar{u}_\Lambda(P') (d_1 \gamma^\mu + i d_2 \sigma^{\mu\nu} q_\nu + d_3 q^\mu) \gamma_5 u_{\Lambda_b}(P), \quad (21)$$

where $P(P')$ is the momentum of the $\Lambda_b(\Lambda)$, $q^2 = (P - P')^2$ is the transformed momentum squared, and g_i , t_i , s_i , and d_i ($i = 1, 2$, and 3) are the transition FFs, which are Lorentz scalar functions of q^2 . The Λ_b and Λ states can be normalized as follows:

$$\langle \Lambda(P') | \Lambda(P) \rangle = 2E_\Lambda(2\pi)^3 \delta^3(P - P'), \quad (22)$$

$$\langle \Lambda_b(v', P') | \Lambda_b(v, P) \rangle = 2v_0(2\pi)^3 \delta^3(P - P'). \quad (23)$$

Comparing Eq. (1) with Eq. (21), we obtain the following relations:

$$g_1 = t_1 = s_2 = d_2 = \left(F_1 + \sqrt{r} F_2 \right), \\ g_2 = t_2 = g_3 = t_3 = \frac{1}{m_{\Lambda_b}} F_2, \\ s_3 = F_2 (\sqrt{r} - 1), \quad d_3 = F_2 (\sqrt{r} + 1), \\ s_1 = d_1 = F_2 m_{\Lambda_b} (1 + r - 2\sqrt{r}\omega), \quad (24)$$

where $r = m_\Lambda^2/m_{\Lambda_b}^2$ and $\omega = (M_{\Lambda_b}^2 + M_\Lambda^2 - q^2)/(2M_{\Lambda_b}M_\Lambda) = v \cdot P'/m_\Lambda$. The transition matrix for $\Lambda_b \rightarrow \Lambda$ can be expressed in terms of the BS wave functions of Λ_b and Λ :

$$\langle \Lambda(P') | \bar{d} \Gamma b | \Lambda_b(P) \rangle = \int \frac{d^4 p}{(2\pi)^4} \bar{\chi}_P(p') \Gamma \chi_P(p) S_D^{-1}(p_2). \quad (25)$$

When $\omega \neq 1$, we can obtain the following expression by substituting Eqs. (11) and (19) into Eq. (25):

$$F_1 = k_1 - \omega k_2, \quad (26)$$

$$F_2 = k_2, \quad (27)$$

where

$$k_1(\omega) = \int \frac{d^4 p}{(2\pi)^4} f_1(p') \phi(p) S_D^{-1}(p_2), \quad (28)$$

$$k_2(\omega) = \frac{1}{1 - \omega^2} \int \frac{d^4 p}{(2\pi)^4} f_2(p') p'_t \cdot v \phi(p) S_D^{-1}. \quad (29)$$

The decay amplitude of $\Lambda_b \rightarrow \Lambda l^+ l^-$ can be rewritten as follows:

$$\mathcal{M}(\Lambda_b \rightarrow \Lambda l^+ l^-) = \frac{G_F \lambda_t}{2\sqrt{2}\pi} \left[\bar{l} \gamma_\mu l \{ \bar{u}_\Lambda [\gamma_\mu (A_1 + B_1 + (A_1 - B_1)\gamma_5) \right. \\ \left. + i \sigma^{\mu\nu} p_\nu (A_2 + B_2 + (A_2 - B_2)\gamma_5)] u_{\Lambda_b} \} \right. \\ \left. + \bar{l} \gamma_\mu \gamma_5 l \{ \bar{u}_\Lambda [\gamma^\mu (D_1 + E_1 + (D_1 - E_1)\gamma_5) \right. \\ \left. + i \sigma^{\mu\nu} p_\nu (D_2 + E_2 + (D_2 - E_2)\gamma_5) \right. \\ \left. + p^\mu (D_3 + E_3 + (D_3 - E_3)\gamma_5)] u_{\Lambda_b} \} \right], \quad (30)$$

where A_i , B_i , D_j , and E_j ($i = 1, 2$ and $j = 1, 2, 3$) are defined as follows:

$$A_i = \frac{1}{2} \left\{ C_9^{\text{eff}} (g_i - t_i) - \frac{2C_7^{\text{eff}} m_b}{q^2} (d_i + s_i) \right\}, \\ B_i = \frac{1}{2} \left\{ C_9^{\text{eff}} (g_i + t_i) - \frac{2C_7^{\text{eff}} m_b}{q^2} (d_i - s_i) \right\}, \\ D_j = \frac{1}{2} C_{10} (g_j - t_j), \quad E_j = \frac{1}{2} C_{10} (g_j + t_j). \quad (31)$$

In the physical region ($\omega = (m_{\Lambda_b}^2 + m_\Lambda^2 - q^2)/(2m_{\Lambda_b}m_\Lambda)$),

the decay rate of $\Lambda_b \rightarrow \Lambda l^+ l^-$ is obtained as follows:

$$\frac{d\Gamma(\Lambda_b \rightarrow \Lambda l^+ l^-)}{d\omega d\cos\theta} = \frac{G_F^2 \alpha^2}{2^{14} \pi^5 m_{\Lambda_b}} |V_{tb} V_{ts}^*|^2 v_l \sqrt{\lambda(1, r, s)} \mathcal{M}(\omega, \theta), \quad (32)$$

where $s = 1 + r - 2\sqrt{r}\omega$, $\lambda(1, r, s) = 1 + r^2 + s^2 - 2r - 2s$

$2rs$, $v_l = \sqrt{1 - \frac{4m_l^2}{sm_{\Lambda_b}^2}}$, and the decay amplitude is expressed as follows [44]:

$$\mathcal{M}(\omega, \theta) = \mathcal{M}_0(\omega) + \mathcal{M}_1(\omega) \cos\theta + \mathcal{M}_2(\omega) \cos^2\theta, \quad (33)$$

where θ is the polar angle, as shown in Fig. 2.

$$\begin{aligned} \mathcal{M}_0(\omega) = & 32m_l^2 m_{\Lambda_b}^4 s(1+r-s)(|D_3|^2 + |E_3|^2) + 64m_l^2 m_{\Lambda_b}^3 (1-r-s)\text{Re}(D_1^* E_3 + D_3 E_1^*) \\ & + 64m_{\Lambda_b}^2 \sqrt{r}(6m_l^2 - M_{\Lambda_b}^2 s)\text{Re}(D_1^* E_1) + 64m_l^2 m_{\Lambda_b}^3 \sqrt{r}(2m_{\Lambda_b} s \text{Re}(D_3^* E_3) + (1-r+s)\text{Re}(D_1^* D_3 + E_1^* E_3)) \\ & + 32m_{\Lambda_b}^2 (2m_l^2 + m_{\Lambda_b}^2 s) \left\{ (1-r+s)m_{\Lambda_b} \sqrt{r} \text{Re}(A_1^* A_2 + B_1^* B_2) \right. \\ & \left. - m_{\Lambda_b} (1-r-s)\text{Re}(A_1^* B_2 + A_2^* B_1) - 2\sqrt{r}(\text{Re}(A_1^* B_1) + m_{\Lambda_b}^2 s \text{Re}(A_2^* B_2)) \right\} \\ & + 8m_{\Lambda_b}^2 \left[4m_l^2 (1-r-s) + m_{\Lambda_b}^2 ((1+r)^2 - s^2) \right] (|A_1|^2 + |B_1|^2) \\ & + 8m_{\Lambda_b}^4 \left\{ 4m_l^2 [\lambda + (1+r-s)s] + m_{\Lambda_b}^2 s [(1-r)^2 - s^2] \right\} (|A_2|^2 + |B_2|^2) \\ & - 8m_{\Lambda_b}^2 \left\{ 4m_l^2 (1+r-s) - m_{\Lambda_b}^2 [(1-r)^2 - s^2] \right\} (|D_1|^2 + |E_1|^2) \\ & + 8m_{\Lambda_b}^5 s v^2 \left\{ -8m_{\Lambda_b} s \sqrt{r} \text{Re}(D_2^* E_2) + 4(1-r+s) \sqrt{r} \text{Re}(D_1^* D_2 + E_1^* E_2) \right. \\ & \left. - 4(1-r-s)\text{Re}(D_1^* E_2 + D_2^* E_1) + m_{\Lambda_b} [(1-r)^2 - s^2] (|D_2|^2 + |E_2|^2) \right\}, \end{aligned} \quad (34)$$

$$\begin{aligned} \mathcal{M}_1(\omega) = & -16m_{\Lambda_b}^4 s v_l \sqrt{\lambda} \left\{ 2\text{Re}(A_1^* D_1) - 2\text{Re}(B_1^* E_1) + 2m_{\Lambda_b} \text{Re}(B_1^* D_2 - B_2^* D_1 + A_2^* E_1 - A_1^* E_2) \right\} \\ & + 32m_{\Lambda_b}^5 s v_l \sqrt{\lambda} \left\{ m_{\Lambda_b} (1-r) \text{Re}(A_2^* D_2 - B_2^* E_2) + \sqrt{r} \text{Re}(A_2^* D_1 + A_1^* D_2 - B_2^* E_1 - B_1^* E_2) \right\}, \end{aligned} \quad (35)$$

$$\mathcal{M}_2(\omega) = 8m_{\Lambda_b}^6 s v_l^2 \lambda (|A_2|^2 + |B_2|^2 + |E_2|^2 + |D_2|^2) - 8m_{\Lambda_b}^4 v_l^2 \lambda (|A_1|^2 + |B_1|^2 + |E_1|^2 + |D_1|^2). \quad (36)$$

The lepton-side forward-backward asymmetry, A_{FB} , is defined as

$$A_{FB} = \frac{\int_0^1 \frac{d\Gamma}{dq^2 dz} dz - \int_{-1}^0 \frac{d\Gamma}{dq^2 dz} dz}{\int_{-1}^1 \frac{d\Gamma}{dq^2 dz} dz}, \quad (37)$$

where $z = \cos\theta$. The "naively integrated" observables are obtained using [17]

$$\langle X \rangle = \frac{1}{q_{\max}^2 - q_{\min}^2} \int_{q_{\min}^2}^{q_{\max}^2} X(q^2) dq^2. \quad (38)$$

We define the integrated A_{FB} as

$$\bar{A}_{FB} = \int_{\hat{q}_{\min}}^{\hat{q}_{\max}} d\hat{q}^2 A_{FB}(\hat{q}^2). \quad (39)$$

where $\hat{q}^2 = q^2/M_{\Lambda_b}^2$. With the aid of the helicity amplitudes of $\Lambda_b \rightarrow \Lambda l^+ l^-$, we can also calculate the hadron forward-backward asymmetry, the lepton-hadron side asymmetry, and the fraction of longitudinally polarized dileptons.

The hadron forward-backward asymmetry has the form

$$\begin{aligned} & A_{FB}^h(q^2) \\ & = \frac{\alpha_\Lambda}{2} \frac{\frac{v_l^2}{2} (\mathcal{H}_P^{11} + \mathcal{H}_P^{22} + \mathcal{H}_{L_p}^{11} + \mathcal{H}_{L_p}^{22}) + \frac{3m_l^2}{q^2} (\mathcal{H}_P^{11} + \mathcal{H}_{L_p}^{11} + \mathcal{H}_{S_p}^{22})}{\mathcal{H}_{\text{tot}}}. \end{aligned} \quad (40)$$

The lepton-hadron side asymmetry has the form

$$A_{FB}^{lh}(q^2) = -\frac{3}{4} \frac{\alpha_\Lambda}{2} \frac{v_l \mathcal{H}_U^{12}}{\mathcal{H}_{\text{tot}}}. \quad (41)$$

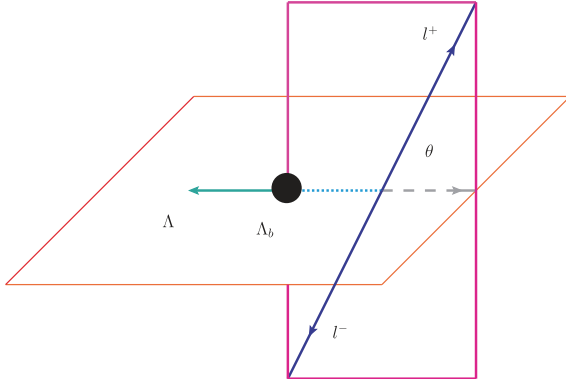


Fig. 2. (color online) Definition of the angle θ in the decay $\Lambda_b \rightarrow \Lambda l^- l^+$.

The fraction of the longitudinally polarized dileptons is expressed by

$$F_L(q^2) = \frac{\frac{v_l^2}{2}(\mathcal{H}_L^{11} + \mathcal{H}_L^{22}) + \frac{m_l^2}{q^2}(\mathcal{H}_U^{11} + \mathcal{H}_L^{11} + \mathcal{H}_S^{22})}{\mathcal{H}_{\text{tot}}}. \quad (42)$$

In Eqs. (40–42), $\mathcal{H}_X^{mm'}(X = U, L, S, P, L_P, S_P, m = 1, 2)$ represent different helicity amplitudes, and \mathcal{H}_{tot} is the total helicity amplitude, $\alpha_\Lambda = 0.642 \pm 0.013$. The explicit expression for $\mathcal{H}_X^{mm'}$ is provided in Ref. [12].

III. NUMERICAL ANALYSIS AND DISCUSSION

In this section, we perform a detailed numerical analysis of $A_{\text{FB}}(\Lambda_b \rightarrow \Lambda l^+ l^-)$. In this study, we take the masses of baryons as $m_{\Lambda_b} = 5.62$ GeV and $m_\Lambda = 1.116$ GeV [45], and the masses of quarks as $m_b = 5.02$ GeV and $m_s = 0.516$ GeV [34, 35, 39]. The variable ω changes from 1 to 2.617, 2.614, 1.617 for e, μ, τ , respectively.

Solving Eqs. (12) and (19) for Λ and Λ_b , we can obtain the numerical solutions of their BS wave functions. In Table 1, we provide the values of α_{self} for different values of κ for Λ and Λ_b with $E_0 = -0.14$ GeV.

From Table 1, we observe that the value of α_{self} is weakly dependent on the value of κ . In Fig. 3, we plot the FFs and FF ratio $R(\omega)$. From this figure, we observe that $R(\omega)$ varies from -0.75 to -0.25 in our model. In Ref. [27], $R(\omega)$ varied from -0.42 to -0.83 in the same ω region, which is in agreement with our result and the estimated value from Refs. [28, 29] mentioned in the Introduction. In the range of $2.43 \leq \omega \leq 2.52$ (corresponding to $M_\Lambda^2 \leq q^2 \leq M_{\Lambda_b}^2$), $R(\omega)$ is about -0.25 . In the same ω region, assuming the FFs have the same dependence on q^2 , the CLEO collaboration measured $R = -0.35 \pm 0.04 \pm 0.04$ in the limit $m_c \rightarrow +\infty$. These results are in good agreement with our research in the same ω region.

In Table 2, we provide \bar{A}_{BF}^l , \bar{A}_{FB}^h , \bar{A}_{FB}^h , and \bar{F}_L for

$\Lambda_b \rightarrow \Lambda \mu^+ \mu^-$ and compare our results with those of other studies. We can observe that these asymmetries differ significantly in different models. Considering these differences, \bar{A}_{FB}^l changes between -0.30 and 0 , \bar{A}_{FB}^h is about 0.1 , \bar{A}_{FB}^h is about -0.25 , and \bar{F}_L changes from 0.3 to 0.6 . Without including the long distance contribution, Ref. [6] provided the integrated forward-backward asymmetry $\bar{A}_{\text{BF}}^l(\Lambda_b \rightarrow \Lambda \mu^+ \mu^-) = -0.1338$. The result of Ref. [7] was $\bar{A}_{\text{BF}}^l(\Lambda_b \rightarrow \Lambda \mu^+ \mu^-) = -0.13(-0.12)$ in the QCD sum rule

Table 1. Values of α_{self} for Λ and Λ_b for different κ values.

κ/GeV^3	Λ	Λ_b
0.045	0.559	0.775
0.047	0.555	0.777
0.049	0.551	0.778
0.051	0.547	0.780
0.053	0.544	0.782
0.055	0.540	0.784

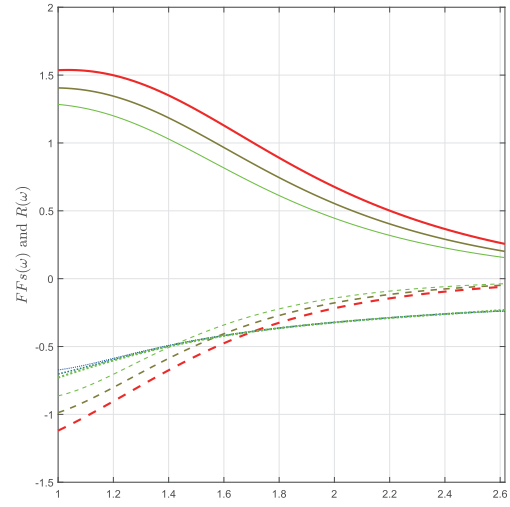


Fig. 3. (color online) Values of F_1 (solid line), F_2 (dash line) and $R(\omega)$ (dot line) as a function of ω (the lines become thicker with the increase in κ).

Table 2. Longitudinal polarization fractions and forward-backward asymmetries for $\Lambda_b \rightarrow \Lambda \mu^+ \mu^-$.

	\bar{A}_{FB}^l	\bar{A}_{FB}^h	\bar{A}_{FB}^h	\bar{F}_L
[6, 7]	-0.13	-	-	0.5830
[8]	8.0×10^{-4}	-	-	-
[12]	-0.286	0.101	-0.288	0.525
[13]	$-0.0122^{+0.0142}_{-0.0073}$	-	-	-
[15]	-0.29 ± 0.05	$0.13^{+0.22}_{-0.03}$	-0.26 ± 0.03	0.4 ± 0.1
[17]	$-0.04^{+0.00}_{-0.01}$	-	-	$0.34^{+0.03}_{-0.02}$
our work	-0.1376 ± 0.0001	0.0576	-0.1613 ± 0.0001	0.3957 ± 0.0002

approach (pole model). Using the covariant constituent quark model with (without) the long distance contribution, Ref. [8] obtained the result $\bar{A}_{\text{FB}}^l(\Lambda_b \rightarrow \Lambda \mu^+ \mu^-) = 1.7 \times 10^{-4}(8 \times 10^{-4})$.

For $q^2 \in [15, 20]$ GeV 2 , the LHCb collaboration provided $A_{\text{FB}}^l(\Lambda_b \rightarrow \Lambda \mu^- \mu^+) = -0.05 \pm 0.09$ in 2015, which was updated to $A_{\text{FB}}^l(\Lambda_b \rightarrow \Lambda \mu^- \mu^+) = -0.39 \pm 0.04$ three years later [4, 5]. In our study, in the same region, the value of $A_{\text{FB}}^l(\Lambda_b \rightarrow \Lambda \mu^- \mu^+)$ changes from -0.44 to -0.35 , which is in good agreement with the most recent experimental data of the LHCb collaboration. With the latest high-precision lattice QCD calculations in the same region, Ref. [46] obtained the values $A_{\text{FB}}^l(\Lambda_b \rightarrow \Lambda \mu^- \mu^+) = -0.344$ in the large ς_u and small ς_d regions (ς_u, ς_d are model parameters [47]) and $A_{\text{FB}}^l(\Lambda_b \rightarrow \Lambda \mu^- \mu^+) = -0.24$ in the large ς_d and small ς_u regions. In Fig. 4, we plot the q^2 -dependence of $A_{\text{FB}}^l(\Lambda_b \rightarrow \Lambda e^- e^+)$, $A_{\text{FB}}^l(\Lambda_b \rightarrow \Lambda \mu^- \mu^+)$, and $A_{\text{FB}}^l(\Lambda_b \rightarrow \Lambda \tau^- \tau^+)$. From Fig. 4, we can observe that $A_{\text{FB}}^l(\Lambda_b \rightarrow \Lambda \mu^+ \mu^-)$ is in good agreement with the lattice QCD calculation in the entire q^2 region [48]. The results of other references results are also shown in Table 3. In Fig. 5, we plot the q^2 -dependence of $A_{\text{FB}}^h(\Lambda_b \rightarrow \Lambda e^- e^+)$, $A_{\text{FB}}^h(\Lambda_b \rightarrow \Lambda \mu^- \mu^+)$, and $A_{\text{FB}}^h(\Lambda_b \rightarrow \Lambda \tau^- \tau^+)$, respectively. For $q^2 \in [15, 20]$ GeV 2 , the LHCb collaboration obtained the value for $\Lambda_b \rightarrow \Lambda \mu^- \mu^+$ as -0.29 ± 0.07 , which is in good agreement our result $-0.2304 \sim -0.0685$. The res-

ults of other references results are also shown in Table 3. In Fig. 6, we plot the q^2 -dependence of $A_{\text{FB}}^{lh}(\Lambda_b \rightarrow \Lambda e^- e^+)$, $A_{\text{FB}}^{lh}(\Lambda_b \rightarrow \Lambda \mu^- \mu^+)$, and $A_{\text{FB}}^{lh}(\Lambda_b \rightarrow \Lambda \tau^- \tau^+)$, respectively. Ref. [12] obtained the value $A_{\text{FB}}^{lh}(\Lambda_b \rightarrow \Lambda \mu^- \mu^+) = 0.145$, which is agreement with our results $0.1257 \sim 0.1555$ in the region $q^2 \in [15, 20]$ GeV 2 . In Fig. 7, we plot the q^2 -dependence of $F_L(\Lambda_b \rightarrow \Lambda e^- e^+)$, $F_L(\Lambda_b \rightarrow \Lambda \mu^- \mu^+)$, and $F_L(\Lambda_b \rightarrow \Lambda \tau^- \tau^+)$, respectively. In the region $q^2 \in [15, 20]$ GeV 2 , the LHCb collaboration obtained the value $F_L(\Lambda_b \rightarrow \Lambda \mu^- \mu^+) = 0.61^{+0.11}_{-0.14}$, which is close to our result of $0.3398 \sim 0.4530$. The results of other references results are also shown in Table 3. From these figures, we observe that all these asymmetries are not very sensitive to the parameters κ and E_0 in our model.

Ref. [17] obtained the naively integrated values $\langle A_{\text{FB}}^l \rangle = -0.19^{+0.00}_{-0.01}$ and $\langle F_L \rangle = 0.6 \pm 0.02$ for $\Lambda_b \rightarrow \Lambda \mu^+ \mu^-$, whereas in our paper, these values are -0.1976 and 0.5681 , respectively. Our results are very close to those of Ref. [17]. In our paper, we obtain $\bar{A}_{\text{FB}}^l = -0.0708 \pm 0.0001(-0.0590 \pm 0.0001)$ and $\bar{A}_{\text{FB}}^h = -0.1604 \pm 0.0001(-0.1541 \pm 0.0002)$ for $\Lambda_b \rightarrow \Lambda e^+ e^- (\Lambda_b \rightarrow \Lambda \tau^+ \tau^-)$. The values given in Ref. [8] are $\bar{A}_{\text{FB}}^l = 1.2 \times 10^{-8}(9.6 \times 10^{-4})$ and $\bar{A}_{\text{FB}}^h = -0.321(-0.259)$, and Refs. [13] and [7] provide $\bar{A}_{\text{FB}}^l = -0.0067$ and $\bar{A}_{\text{FB}}^l = -0.04$ for $\Lambda_b \rightarrow \Lambda \tau^+ \tau^-$. Comparing the values in these theoretical approaches, we observe that the asymmetries may vary widely among the

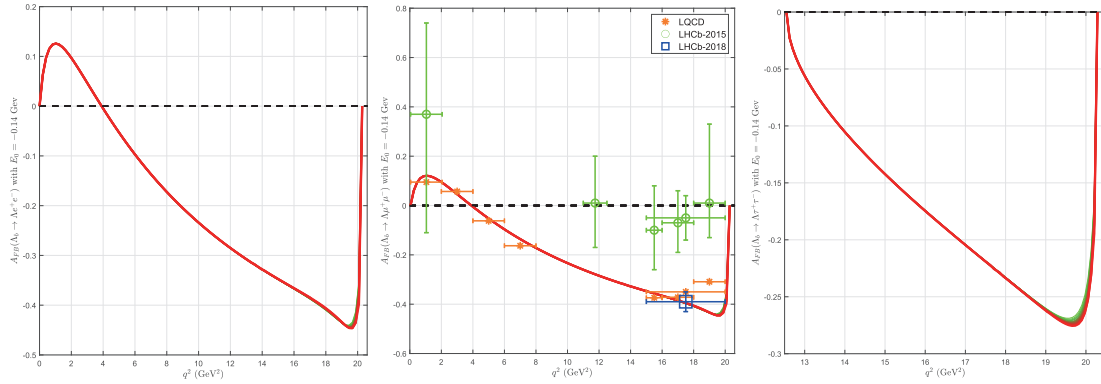


Fig. 4. (color online) Values of $A_{\text{FB}}(\Lambda_b \rightarrow \Lambda l^+ l^-)$ as a function of q^2 for different values of κ as shown in Table 1.

Table 3. Longitudinal polarization fractions and forward-backward asymmetries for $\Lambda_b \rightarrow \Lambda \mu^+ \mu^-$ in $q^2 \in [15, 20]$ GeV 2 .

—	$A_{\text{FB}}^l[15, 20]$	$A_{\text{FB}}^{lh}[15, 20]$	$A_{\text{FB}}^h[15, 20]$	$F_L[15, 20]$
LHCb [4, 5]	-0.39 ± 0.04	—	-0.29 ± 0.07	$0.61^{+0.11}_{-0.14}$
[6, 7]	$-0.40 \sim -0.25$	—	—	$0.37 \sim 0.62$
[8]	$-0.24 \sim -0.13$	—	> -0.308	—
[12]	-0.40	0.145	-0.29	0.38
[13]	$-0.075 \sim -0.017$	—	—	—
[17]	$-0.34^{+0.01}_{-0.02}$	—	—	$0.4^{+0.01}_{-0.02}$
[48]	$-0.350(13)$	—	-0.2710 ± 0.0092	0.409 ± 0.013
our work	$-0.44 \sim -0.35$	$0.1257 \sim 0.1555$	$-0.2304 \sim -0.0685$	$0.3398 \sim 0.4530$

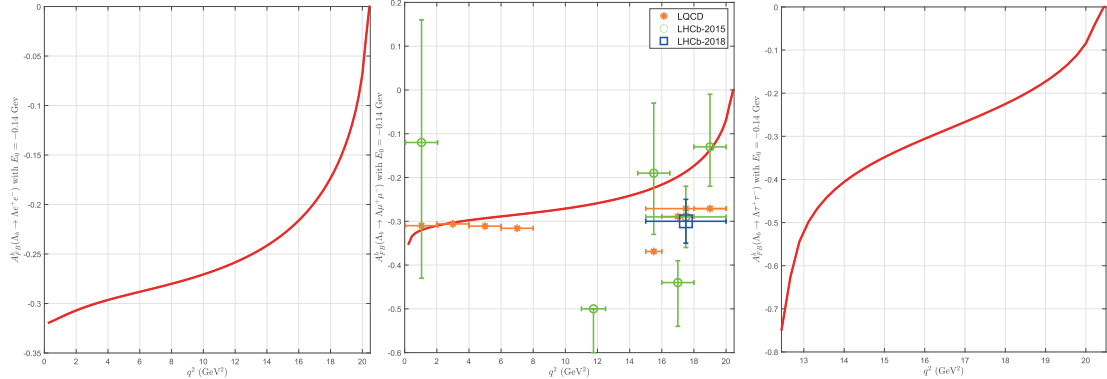


Fig. 5. (color online) Values of $A_{FB}^h(\Lambda_b \to \Lambda l^+ l^-)$ as a function of q^2 for different values of κ as shown in Table 1.

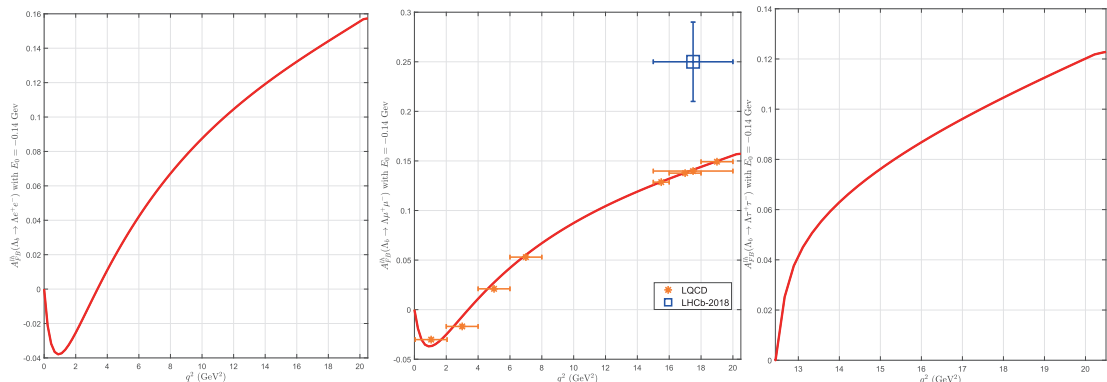


Fig. 6. (color online) Values of $A_{FB}^h(\Lambda_b \to \Lambda l^+ l^-)$ as a function of q^2 for different values of κ as shown in Table 1.

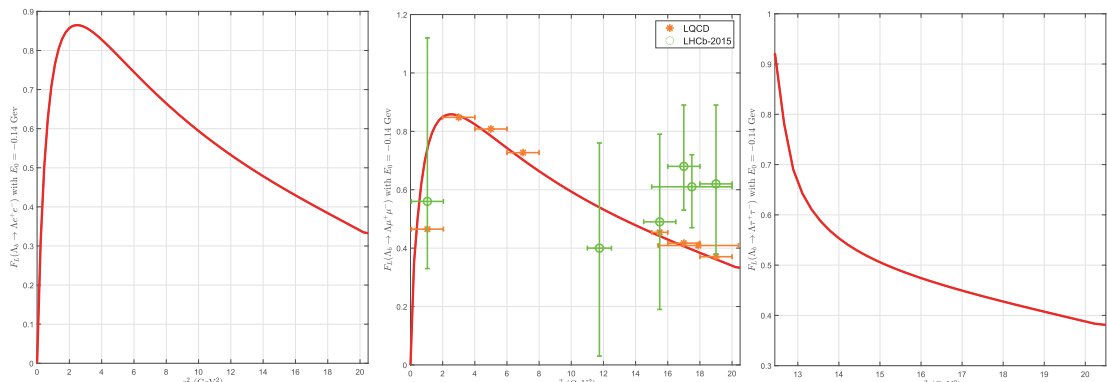


Fig. 7. (color online) Values of $F_L(\Lambda_b \to \Lambda l^+ l^-)$ as a function of q^2 for different values of κ as shown in Table 1.

theoretical models because the FFs in these models are different.

IV. SUMMARY AND CONCLUSIONS

In this study, we use the BSE to study the forward-backward asymmetries in the rare decays $\Lambda_b \to \Lambda l^+ l^-$ in a covariant quark-diquark model. In this picture, $\Lambda_b(\Lambda)$ is considered a bound state of a $b(s)$ -quark and a scalar diquark.

We establish the BSE for the quark and scalar diquark system and then derive the FFs of $\Lambda_b \to \Lambda$. We solve the BS equation of this system and then provide the values of

the FFs and R . We observe that the ratio R is not a constant, which is in agreement with Ref. [26] and the pQCD scaling law [23–25]. Using these FFs, we calculate the forward-backward asymmetries A_{FB}^l , A_{FB}^{lh} , and A_{FB}^h and longitudinal polarization fractions F_L and the integrated forward-backward asymmetries \bar{A}_{FB}^l , \bar{A}_{FB}^{lh} , and \bar{A}_{FB}^h as well as \bar{F}_L for $\Lambda_b \to \Lambda l^+ l^- (l = e, \mu, \tau)$. Comparing with other theoretical studies, we observe that the FFs are different; thus, these asymmetries are different. The long distance contributions are not included in this paper. They will be considered in our future research to compare the experimental data more exactly.

References

- [1] T. Aaltonen *et al.* (CDF collaboration), *Phys. Rev. Lett.* **107**, 201802 (2011)
- [2] R. Aaij *et al.* (LHCb collaboration), *Phys. Lett. B* **725**, 25 (2013)
- [3] R. Aaij *et al.* (LHCb collaboration), *Phys. Rev. Lett.* **123**, 031801 (2019)
- [4] R. Aaij *et al.* (LHCb collaboration), *JHEP* **06** 115 (2017); **09**, 145 (2018)
- [5] R. Aaij *et al.* (LHCb collaboration), *JHEP* **09**, 146 (2018)
- [6] C. H. Chen and C. Q. Geng, *Phys. Rev. D* **64**, 074001 (2001)
- [7] C. H. Chen and C. Q. Geng, *Phys. Lett. B* **516**, 327 (2001)
- [8] T. Gutsche, M. A. Ivanov, J. G. Körner *et al.*, *Phys. Rev. D* **87**, 074031 (2013)
- [9] T. M. Aliev, V. Bashir, and M. Savci, *Nucl. Phys. B* **709**, 115 (2005)
- [10] T. Mannel and Y. M. Wang, *JHEP* **12**, 067 (2011)
- [11] L. Mott and W. Roberts, *Int. J. Mod. Phys. A* **27**, 1250016 (2012)
- [12] R. N. Faustov and V. O. Galkin, *Phys. Rev. D* **96**(5), 053006 (2017)
- [13] Y. M. Wang, Y. Li, and C. D. Lü, *Eur. Phys. J. C* **59**, 861 (2009)
- [14] Y. M. Wang and Y. L. Shen, *JHEP* **02**, 179 (2016)
- [15] P. Böer, T. Feldmann, and D. van Dyk, *JHEP* **01**, 155 (2015)
- [16] L. Mott and W. Roberts, *Int. J. Mod. Phys. A* **30**, 1550172 (2015)
- [17] R. M. Wang, Y. G. Xu, C. Hua *et al.*, *Phys. Rev. D* **103**, 013007 (2021)
- [18] T. Mannel, W. Roberts, and Z. Ryzak, *Nucl. Phys.* **355**, 38 (1991)
- [19] CLEO Collaboration, *Phys. Rev. Lett.* **94**, 191801 (2005)
- [20] T. Mannel and S. Recksiegel, *J. Phys. G: Nucl. Part. Phys.* **24**, 979 (1998)
- [21] C. S. Huang and C. Q. Geng, *Phys. Rev. D* **63**, 114024 (2001)
- [22] T. M. Aliev, A. Özpineci, and M. Savci, *Nucl. Phys.* **649**, 168 (2003)
- [23] G. P. Lepage and S. J. Brodsky, *Phys. Rev. D* **22**, 2157 (1980)
- [24] S. J. Brofsky and G. R. Farrar, *Phys. Rev. D* **11**, 1309 (1975)
- [25] C. F. Perdrisat, V. Punjabi, and M. Vanderhaeghen, *Prog. Part. Nucl. Phys.* **59**, 694 (2007)
- [26] X. H. Guo and T. Huang, *Phys. Rev. D* **53**, 4946 (1996)
- [27] C. S. Huang and H. G. Yan, *Phys. Rev. D* **59**, 114022 (1999)
- [28] L. L. Liu, X. W. Kang, Z. Y. Wang *et al.*, *Chin. Phys. C* **44**, 083107 (2020)
- [29] L. L. Liu, C. Wang, X. W. Kang *et al.*, *Eur. Phys. J. C* **80**, 193 (2020)
- [30] N. G. Deshande, X. G. He, and J. Trampetic, *Phys. Lett. B* **367**, 362-368 (1996)
- [31] E. Golowich and S. Pakvasa, *Phys. Rev. D* **51**, 1215 (1995)
- [32] X. H. Guo and T. Muta, *Phys. Rev. D* **54**, 4629 (1996)
- [33] Liang-Liang Liu, Chao Wang, and Xin-Heng Guo, *Chin. Phys. C* **42**, 103106 (2018)
- [34] Liang-Liang Liu, Chao Wang, Ying Liu *et al.*, *Phys. Rev. D* **95**, 054001 (2017)
- [35] Y. Liu, X. H. Guo, and C. Wang, *Phys. Rev. D* **91**, 016006 (2015)
- [36] X. H. Guo and H. K. Wu, *Phys. Lett. B* **654**, 97 (2007)
- [37] M. H. Weng, X. H. Guo, and A. W. Thomas, *Phys. Rev. D* **83**, 056006 (2011)
- [38] X. H. Guo and X. H. Wu, *Phys. Rev. D* **76**, 056004 (2007)
- [39] L. Zhang and X. H. Guo, *Phys. Rev. D* **87**, 076013 (2013)
- [40] R. Jakob, P. Kroll, M. Schürmann *et al.*, *Z. Phys. A* **347**, 109 (1993)
- [41] K. Azizi, S. Kartal, A. T. Olgun *et al.*, *JHEP* **10**, 118 (2012)
- [42] M. J. Aslam, C. D. Lü, and Y. M. Wang, *Phys. Rev. D* **79**, 074007 (2009)
- [43] W. J. Li, Y. B. Dai, and C. S. Huang, *Eur. Phys. J. C* **40**, 565 (2005)
- [44] A. K. Giri and R. Mohanta, *Eur. Phys. J. C* **45**, 151 (2006)
- [45] P. A. Zyla *et al.* (Particle Data Group), *Prog. Theor. Exp. Phys.* **2020**, 083C01 (2020)
- [46] Q. Y. Hu, X. N. Li, and Y. D. Yang, Arxiv: 1701.04029[hep-ph]
- [47] Q. Y. Hu, X. Q. Li, and Y. D. Yang, *Eur. Phys. J. C* **77**, 190 (2017)
- [48] W. Detmold and S. Meinel, *Phys. Rev. D* **93**, 074501 (2016)